

Article

Effects of Biotic and Abiotic Factors on Biomass Conversion and Expansion Factors of Natural White Birch Forest (*Betula platyphylla* Suk.) in Northeast China

Yanrong Wang [†], Zheng Miao [†], Yuanshuo Hao, Lihu Dong ^{* } and Fengri Li ^{}

Key Laboratory of Sustainable Forest Ecosystem Management-Ministry of Education, School of Forestry, Northeast Forestry University, Harbin 150040, China

* Correspondence: lihudong@nefu.edu.cn; Tel.: +86-451-82191751

† These authors contributed equally to this work.

Abstract: Biomass conversion and expansion factors ($BCEF_s$) are widely utilized in national and regional biomass estimates and greenhouse gas reporting, as they can be used to directly transform the stocking volume into biomass. In this study, the power function was used as the basic model form with biotic variables, and abiotic variables were considered to improve the fitting results. Then, the random effects parameters were also introduced into the models to describe the variation of $BCEF_s$ among different forest management units. Random sampling strategies were applied to calibrate the random effects. The results showed that the stocking volume exhibited a negative proportional relationship in the stem $BCEF$ ($BCEF_{st}$), the root $BCEF$ ($BCEF_{ro}$) and the total tree $BCEF$ ($BCEF_{to}$) models, and the quadratic mean diameter exhibited a positive proportional relationship in the branch $BCEF$ ($BCEF_{br}$) and the foliage $BCEF$ ($BCEF_{fol}$) models. In addition, the fitting effect of generalized models with abiotic predictors was superior to that of the basic models. Considering the effects of abiotic variables on the $BCEF_s$ of each component, the results showed that $BCEF_{st}$ and $BCEF_{to}$ decreased as the mean annual precipitation increased; $BCEF_{br}$ increased as the annual temperature increased; $BCEF_{fol}$ gradually decreased as the elevation increased; and $BCEF_{ro}$ first increased with increasing mean annual temperature and then declined. In conclusion, abiotic factors explained the variation in $BCEF_s$ for the biomass components of the natural white birch forest. Although the fitting effect of generalized models with abiotic predictors was superior to that of the basic models, the mixed-effects model was preferable for modeling the $BCEF_s$ of each component. In addition, the prediction precision of the mixed-effects models enhanced gradually with increasing sample size, and the selection of eight plots for calibration and prediction based on the mixed-effects model was the best sampling strategy in this study of a natural white birch forest.

Keywords: natural white birch forest; $BCEF_s$; mixed effects model; topographic conditions; climate variables



Citation: Wang, Y.; Miao, Z.; Hao, Y.; Dong, L.; Li, F. Effects of Biotic and Abiotic Factors on Biomass Conversion and Expansion Factors of Natural White Birch Forest (*Betula platyphylla* Suk.) in Northeast China. *Forests* **2023**, *14*, 362. <https://doi.org/10.3390/f14020362>

Academic Editor: Juan A. Blanco

Received: 31 December 2022

Revised: 6 February 2023

Accepted: 8 February 2023

Published: 11 February 2023



Copyright: © 2023 by the authors. Licensee MDPI, Basel, Switzerland. This article is an open access article distributed under the terms and conditions of the Creative Commons Attribution (CC BY) license (<https://creativecommons.org/licenses/by/4.0/>).

1. Introduction

As one of the crucial components of terrestrial ecosystems, forest ecosystems play a significant role in the global greenhouse gas (GHG) balance because they can absorb and store more carbon and mitigate the global environmental pollution caused by global warming [1–3]. The method for estimating forest biomass carbon is the conversion of widely available biomass into biomass carbon using the average carbon concentration for forests [4–6]. Usually, a value of 45% or 50% is used as the common carbon concentration for forests. This indicates that the average carbon concentration is generally constant. Therefore, the assessment of biomass leads to an accurate biomass calculation of carbon sequestration in the ecosystem. In the background of increasing concentrations of CO₂ and global warming [7], improving the accuracy of biomass estimation and using appropriate estimation methods are essential for the assessment of biomass [8,9].

Stand biomass estimation methods mainly include biomass allometric equations based on measured attributes and biomass assessments using biomass conversion and expansion factors ($BCEF_s$) [10–13]. However, there are two drawbacks to the allometric equation: (1) the variables influencing the stand biomass cannot be taken into account comprehensively and the main independent variables are diameter, height, age or crown, based on previous research [6,14–21]; and (2) we cannot use allometric equations for large-scale assessments, because they are based on individual tree diameter at breast height (DBH), height (H) and crown width (CW) that are not available in forest inventories of large-scale measurements, especially H and CW . These two problems are common in most forest types, especially in natural white birch forests.

Four parameters are normally used to convert stand biomass values: biomass conversion and expansion factors ($BCEF_s$), wood density (WD), biomass expansion factors ($BEFs$) and root-to-shoot ratio (root: shoot ratio, R/S) [7,22]. However, compared with other conversion factors, the $BCEF_s$ of each component are widely used in large-scale forest carbon storage calculations [10,23]. $BCEF$ is considered the correlation between the stocking volume and the biomass of each component and is defined as the ratio of biomass of various organs to the stocking volume; it can be used to directly convert the stocking volume data into the biomass of various organs. $BCEF_s$ can be divided into two forms: constant $BCEF_s$ defined from the mean or range of $BCEF_s$ for a certain forest type, and $BCEF_s$ which is estimated through equation-based stand factors [11,24,25]. However, a large number of studies have shown that $BCEF_s$ values can vary according to the origin and type of species, climate change, tree size, and age [20,23,25].

Assuming a constant $BCEF_s$ can lead to large estimation errors [26,27]. To reduce the uncertainty in the biomass and carbon storage estimation, variable $BCEF_s$ have been used in numerous studies to account for variation in the allometry and ability of carbon storage and fixation.

Age-sensitive exponential functions were developed in earlier studies to predict $BCEF_s$ for biomass components; however, additional studies showed that the stand age could not explain differences in stand growth conditions and stand biology [28,29]. An increasing number of researchers have introduced the factors of stand growth, stocking volume, quadratic mean diameter at breast height, and stand average height into the $BCEF_s$ model, but their analyses did not consider the effect of abiotic factors on $BCEF_s$ [30,31]. With further study, some scholars have also suggested that abiotic factors such as site index, climate, and forest management intensity profoundly impact $BCEF_s$, indicating that abiotic factors should be considered in the $BCEF_s$ model [21,23,32].

In recent years, researchers used nonlinear mixed-effects models to construct forest models [33–36]. Usually, datasets required for modeling $BCEF_s$ were derived from measurements of sample plots randomly distributed in different regions, so that the nested structure led to a high correlation between different regions and sample plots in different regions [35,37,38]. In this case, the performance of the nonlinear mixed-effects model surpasses the performance of ordinary least-squares regression by adding random effects to the model [39,40]. Moreover, even though mixed-effects models are used to estimate random effects, applying different strategies to confirm the optimal number of sampling stands to achieve the required level of precision is necessary, so that the cost and time for data collection can be reduced for forest managers [41,42].

White birch (*Betula platyphylline* Suk.) has strong natural regeneration and is the main component species of forest vegetation in northeast China [43,44]. It can often be found in pure forests or mixed forests with other coniferous and broad-leaved species, and is a major pioneer tree species in the process of forest succession in natural forests [45,46]. Natural white birch forests were formed after the disturbance of the native top community of broad-leaved red pine forests in early northeastern China, which played a transitional role in community succession [43,45]. Natural birch forests are important for soil and water conservation, improving soil fertility, storing carbon, and regulating and maintaining an ecological balance in northeast China [44]. However, there have been relatively few reports

on the $BCEF_s$ of natural white birch forests in China. Although many models of $BCEF_s$ have been developed for other tree species, they were based on small sample size, and the generalizability was poor. In addition, studies have shown that the carbon neutrality of white birch mainly occurs in living trees, so it is crucial to select suitable forest biomass estimation methods [47,48].

The objectives of the study were as follows: (1) to present a generalized model for $BCEF_s$ including abiotic factors; (2) to quantify changes in $BCEF_s$ on regional scales using a mixed-effects model; (3) to compare the performances of the basic model, generalized model, and mixed-effects model, examining them with the jackknife approach and determining an appropriate sample size that considers both prediction accuracy and sampling cost; and (4) to analyze the $BCEF_s$ differences among different conditions, including different biotic and abiotic conditions. In summary, our goal was to determine the reason for $BCEF_s$ differences and obtain a practical model to predict natural white birch carbon sinks.

2. Materials and Methods

2.1. Study Area

The study area is distributed in northeast China across three mountains in Heilongjiang Province and Jilin Province: the Daxing'an Mountains ($121^{\circ}12' \sim 127^{\circ}00'$ E, $50^{\circ}10' \sim 53^{\circ}33'$ N, 100~1400 m a.s.l.), Xiaoxing'an Mountains ($127^{\circ}42' \sim 130^{\circ}14'$ E, $46^{\circ}28' \sim 49^{\circ}21'$ N, 600~1000 m a.s.l.) and Changbai Mountains ($121^{\circ}08' \sim 134^{\circ}00'$ E, $38^{\circ}46' \sim 47^{\circ}30'$ N, 500~1000 m a.s.l.). The study area is found in the temperate continental climate zone. The annual average temperature in northeast China varies from -7 to 6°C , and the annual precipitation varies from 179 to 1189 mm (Figure 1).

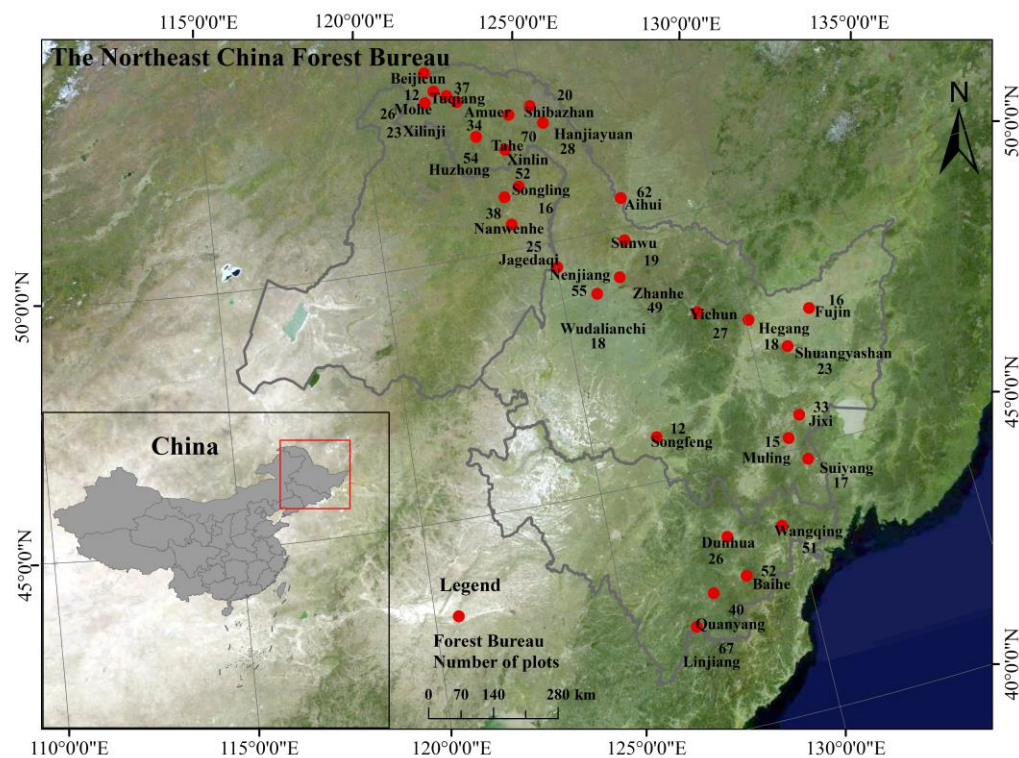


Figure 1. Study area showing the sample plot locations.

2.2. Forest Survey and Design Data

The survey data were from rectangular permanent sample plots (PSPs) in natural white birch forests in China's National Forest Inventory across the Daxing'an Mountains, Xiaoxing'an Mountains and Changbai Mountains, northeast China (Figure 1). The rectangular PSPs were managed by 31 different forestry management units (FMUs). This

subsample of data used for the analysis included 1035 plots. A total of 723 PSPs in 24 forest bureaus of Heilongjiang Province were studied during the period from 2005 to 2010, and measurements from 412 other PSPs located in seven forest bureaus of Jilin Province were taken between 1990 and 2010. In total, the inventory data included 173 unique plots and 962 cases repeated (second) measurements. Each plot comprised an area of 30 m × 20 m. The data in this study were surveyed in the field using a diameter tape and a Blume–Leiss Hypsometer. The DBH of all standing living trees with DBH ≥ 5 cm in the sample plot was measured and the tree height of three to five standard trees was measured in each plot. DBH and H were used in the calculation of stand variables.

In addition, the topographic factors such as elevation (ELV/m), slope (°) and slope direction (SLP) were recorded for each sample plot. To facilitate the study of topographic factors, they were converted into continuous variables for calculation in this study [49,50]. Table 1 lists the specific calculation formulas and descriptions for the stand variables and topographic factors used in our study. The descriptive statistics of stand variables and topographic conditions are listed in Table 2.

Table 1. Units and descriptions of available variables for models of biomass conversion and expansion factors.

Attribute	Variable	Units	Descriptions
Stand attributes	H_a	m	The average tree height is the average height of 3 to 5 standard trees in the stand.
	D_q	cm	The quadratic mean diameter: $\sqrt{\sum DHB_i^2/n}$,
	D_{dom}	cm	The quadratic mean diameter of dominant species
	G	$m^2 \text{ hm}^{-2}$	The quadratic mean dominant diameter: $\sum_1^n \pi DBH_i^2/4000$
	NH_a	$\text{tree} \cdot \text{hm}^{-2}$	The number of trees per hectare
	M	$m^3 \text{ hm}^{-2}$	stand volume: $M = \sum v_i$; v_i is individual tree volume: $v_i = aDBH^b$ a and b are model coefficients based on [51]
	W_i	$\text{Mg} \text{ hm}^{-2}$	Biomass: $W_i = aDBH^b$; a and b are model coefficients based on Dong, et al. [16]
Topographic conditions	$BCEF_i$	$\text{Mg} \text{ m}^3$	Biomass conversion and expansion factor: $BCEF_i = W_i/M$
	ELV	m	Elevation
	SL		The slope rate value: $SL = \tan(SLP)$
	SLP		Slope direction
	SLC		The slope rate value multiplied by the slope cosine value.
	SLS		The slope rate value multiplied by the slope sine value

2.3. Climate Data

A large number of studies have shown that climate factors have significant effects on the $BCEF_s$ of larch, eucalyptus and other tree species [23,52]. To further investigate the influence of climate on the $BCEF_s$ of different components of natural white birch forests, the ClimateAP database was used to obtain all the PSPs, for which the altitude ranged from 122 to 1150 m, longitude ranged from 121°64'46'' E to 31°01'56'' E, and latitude ranged from 41°63'98'' N to 453°47'75'' N [53,54]. ClimateAP is available at UBC server in both desktop and Google Map-based web formats. It is a software application for extracting climate data for past and future periods in the Asia-Pacific region, which can output scale-free and downscaled monthly, seasonal, and annual climate variables for the corresponding years based on latitude, longitude, and elevation interpolation [54]. The downscaled grids of climate data were provided at the resolution of about 4 × 4 km [54]. In this study, sixteen annual climatic variables were used as candidate bioclimatic variables for model fitting. The observations of the variables were summarized for the annual climatic variables averaged from 1981 to 2010. The names and abbreviations of the full list of climate variables used for analysis are shown in Table 3.

Table 2. Descriptive statistics of the stand variables and topographic conditions for birch.

Attribute	Variable	Mean	Min.	Max.	SD.
Stand attributes	D_g	13.51	5.50	27.20	4.91
	G	12.64	0.55	33.19	7.08
	H_a	12.52	5.00	22.70	3.44
	M	82.62	2.50	247.30	54.01
	N	1125.20	200.00	3467.00	617.46
	D_q	12.12	5.50	21.70	3.39
	$BCEF_{st}$	0.5687	0.4549	0.7183	0.0449
	$BCEF_{br}$	0.1076	0.0524	0.1785	0.0248
	$BCEF_{fol}$	0.0255	0.0180	0.0322	0.0026
	$BCEF_{ro}$	0.2117	0.1610	0.2907	0.0235
Topographic conditions	$BCEF_{to}$	0.9139	0.7473	1.1250	0.0719
	ELV	582	122	1150	200
	SL	0.0888	0	0.488	0.0723
	SLP	5.0473	0	26.000	4.0071
	SLC	0.0106	−0.364	0.404	0.0785
	SLS	0.0016	−0.330	0.488	0.0827

Note: st: stem, fol: foliage, br: branch, ro: root, to: total, SD: the standard deviation.

Table 3. List of abbreviations and explanation of available climate variables for $BCEF_s$ models. The mean values of climate variables over each survey interval (30 years) for the period from 1981 to 2010 were used.

Variable	Units	Description
MAT	°C	Mean annual temperature
$MWMT$	°C	Mean warmest month temperature
$MCMT$	°C	Mean coldest month temperature
$DD.0$	°C	Degree-days below 0 °C, chilling degree-days
$DD.5$	°C	Degree-days above 5 °C, growing degree-days
$DD.18$	°C	Degree-days below 18 °C, heating degree-days
$DD.18.1$	°C	Degree-days above 18 °C, cooling degree-days
TD	°C	Temperature difference between $MWMT$ and $MCMT$, or continentality (°C)
MAP	mm	Mean annual precipitation
AHM	—	Annual heat $(MAT + 10)/(MAP/1000)$
$NFFD$		The number of frost-free days
PAS	mm	Precipitation as snow (mm) between August in previous year and July in current year
EMT	°C	Extreme minimum temperature over 30 years
EXT	°C	Extreme maximum temperature over 30 years
$Eref$	mm	Hargreaves reference evaporation
CMD	mm	Hargreaves climatic moisture deficit

2.4. Methods

2.4.1. Basic and Generalized Model

Power functions, hyperbolic functions and reciprocal equations have been widely used to simulate the $BCEF_s$ of each component [10,12,29]. Basic models were implemented in *R* with the package “*nls*”. Based on a preliminary analysis, the power function was determined as the basic model. The equation is as follows:

$$BCEF_i = a X^b \quad (1)$$

where X is the characteristic (D_q , H_a , M or G), i denotes each component (stem, branch, foliage, root or total), and a and b are model coefficients. We used iterative least-squares regression to implement the function [55,56].

In addition to biotic factors, $BCEF_i$ are affected by climate factors and topographic factors [21,23,52]. Therefore, to evaluate the variation in $BCEF_i$ due to different abiotic

factors, generalized models of biomass constituents were developed by reparameterization. The coefficient b was not influenced by abiotic factors in the preliminary analysis. Therefore, we adopted coefficient a of the generalized models, which was represented as a linear function of abiotic variables [57,58]:

$$a = a_0 + \sum a_i x_i \quad (2)$$

where a_0 is the intercept; a_i are the coefficients; and x_i are the environmental factors, including topographic variables and climate variables. The study included 21 abiotic factors with 16 climate variables and five topographic variables. To unify the dimensions, MAP , AHM and ELV were divided by 1000, and MAT was standardized: $MAT_{standardized} = (MAT - (-7))/(6 - (-7))$. The average annual temperature range is -7 to 6 °C in northeast China. In addition, to avoid multicollinearity among variables and a decline in model accuracy due to the redundancy of independent variables, the variance inflation factor (VIF) was used to preselect all concomitant variables in the study. Covariates with statistically significant VIF ($p < 0.05$) and $VIF < 5$ were retained in the model [59]. The parameters of the prediction models were estimated by R , and a t test was performed on all parameters [53].

2.4.2. Mixed-Effects Models

Since the survey data were from 31 different forest management units, we used nonlinear mixed-effects models to develop $BCEF_i$. Both random- and fixed-effect variables were included in the mixed-effects models. The general expression of the nonlinear mixed-effects model is shown in Equation (3). The mixed-effects model of each component was implemented in R using the package “nlme”, and the parameter estimation of the model was based on the restricted maximum likelihood ($REML$) method [41]. Although the location and number of random effect parameters were unknown, we assumed that all parameters had random effects, and all models had different random effect parameter combinations [3]. In the converged model, by comparing the Bayesian information criterion (BIC), Akaike information criterion (AIC), and $-2\log$ -likelihood ($-2LL$), the optimal random effect parameters were determined [3,41] as follows:

$$y_i = f(\Phi_i, x_i) + e_i, \quad i = 1, 2, \dots, M \quad (3)$$

where y_i represents the vector of response variable ($BCEF_i$) in the i -th FMU ; M is the number of $FMUs$; f is a nonlinear function of the FMU -specific parameter vector Φ_i and predictor variable x_i ; and e_i is the within- FMU independent random error vector, which follows a multivariate normal distribution with a mean value vector of 0 and variance-covariance matrix of R . Φ_i is given as:

$$\Phi_i = A_i \beta + B_i b_i; b_i \sim N(0, D) \quad (4)$$

where β is a p -dimensional fixed-effect parameter vector; b_i is a q -dimensional random-effect parameter vector, which is assumed to have a multivariate normal distribution with a mean value vector of 0 and variance-covariance matrix of D ; and A_i , and B_i are the incidence matrices of the appropriate dimensions of fixed- and random effect, consisting of 0 or 1.

$$e_i \sim N\left(0, \sigma^2 G_i^{0.5} \Gamma_i G_i^{0.5}\right) \quad (5)$$

σ^2 is the scaling factor of error dispersion, which is derived from the residuals of the estimated model. G_i is a matrix that represents the heterogeneity of the residual variance within- FUM and its diagonal elements were provided by the variance function. Through the preliminary data analysis, we found no heteroscedasticity in the mixed-effects model, so that the unit matrix G_i was set by default to 1. Matrix Γ_i represents the residual correlation within the FUM , which was defined as the identity matrix I in our study.

2.4.3. Model Assessment and Calibration Prediction

The root mean square error (*RMSE*), *AIC*, and adjusted coefficient of determination (R_a^2) were used as the main criteria for evaluating the fitting performance. The model with the largest R_a^2 , and the smallest *RMSE* and *AIC*, were selected as the final model [6,15,16].

$$R_a^2 = 1 - \left(\frac{n-1}{n-p} \right) \frac{\sum_{i=1}^n (y_i - \hat{y}_i)^2}{\sum_{i=1}^n (y_i - \bar{y})^2} \quad (6)$$

$$RMSE = \sqrt{\frac{\sum_{i=1}^n (y_i - \hat{y}_i)^2}{n-p-1}} \quad (7)$$

$$AIC = -2LL + 2p \quad (8)$$

In this study, we fitted the models using the whole dataset and used the jackknife technique to test the predictive performance of the models [60]. Mean absolute error (*MAE*), mean absolute percent error (*MAPE%*) and model efficiency (*FE*) were used as the main criteria for evaluating the performance of model validation.

$$MAE = \frac{\sum_{i=1}^n |y_i - \hat{y}_i|}{n} \quad (9)$$

$$MAPE = \frac{\sum_{i=1}^n |y_i - \hat{y}_i|}{n} \times 100 \quad (10)$$

$$FE = 1 - \frac{\sum_{i=1}^n (y_i - \hat{y}_i)^2}{\sum_{i=1}^n (y_i - \bar{y})^2} \quad (11)$$

The fixed-effects parameters of the nonlinear mixed-effects model can be tested in the traditional way, while the random-effects parameters require some a priori information. The calculation of random-effects parameters in the mixed-effects models was based on the best linear unbiased predictions (*BLUPs*) method [61–63]. The specific computation formula is as follows:

$$\hat{b}_k = \hat{D}Z_k^T (Z_k \hat{D}Z_k^T + \hat{R}_k)^{-1} \hat{e}_k \quad (12)$$

where \hat{b}_k is a vector of random effects parameters of sampled *FUM* *k* calculated by all sampled plots; *D* is the variance–covariance matrix estimated in the modeling process; \hat{R}_k is the corresponding variance–covariance matrix of within-group errors; Z_k is the matrix of the partial derivatives of the nonlinear function with respect to its random parameters; and \hat{e}_k is the error term of observed *BCEF_s* response and predicted by the fixed-effects parameters in the mixed-effects model.

3. Results

3.1. Basic and Generalized Model

The influence of the stand variables in Table 2 on the *BCEF_s* of different compositions was assessed based on Equation (1); the variables *M*, which were strongly correlated with *BCEF_{st}*, *BCEF_{ro}* and *BCEF_{to}* were chosen as the basic variation to establish the basic model of *BCEF_{st}*; *BCEF_{ro}* and *BCEF_{to}*, and the variables *D_q*, which were strongly correlated with *BCEF_{fol}*, and *BCEF_{br}* was selected as basic variation to fit the basic model of *BCEF_{fol}*, and *BCEF_{br}*. The fit statistics based on power functions for *BCEF_s* of biomass components are shown Table 4.

To accurately reflect the influence of abiotic factors on the *BCEF_s* of different components, we introduced abiotic factors into the basic models to improve the basic models and build generalized models. No noticeable correlation was detected among the independent variables in the generalized models, and the *VIF* values of all the variables were less than 5, indicating collinearity in these five *BCEF_s* models. Table 5 shows the final forms of the generalized models, where a_1 and a_2 are the coefficients to be estimated in the generalized model.

Table 4. Fitting Statistics of the Basic Model.

Predictors	Component	Component	$BCEF_{br}$	$BCEF_{fol}$	$BCEF_{ro}$	$BCEF_{to}$
		M (m ³ hm ⁻²)	D_q (cm)	D_q (cm)	M (m ³ hm ⁻²)	M (m ³ hm ⁻²)
parameter	a	0.668	0.021	0.018	0.284	1.019
	b	-0.040	0.662	0.134	-0.073	-0.027
statistical index	R_a^2	0.206	0.692	0.155	0.365	0.104
	-2LL	-3719.254	-5935.322	-9577.212	-5307.534	-2732.799
	AIC	-3713.254	-5929.322	-9571.212	-5301.534	-2726.799
	RMSE	0.040	0.014	0.001	0.019	0.065

Table 5. Generalized models of biomass conversion and expansion factor of each component.

Generalized Model	Model
$BCEF_{st} = (a + a_1 \times MAP/1000) \times M^b$	(1)
$BCEF_{br} = (a + a_1 \times AHM/1000) \times Dq^b$	(2)
$BCEF_{fol} = (a + a_1 \times ELV/1000) \times Dq^b$	(3)
$BCEF_{ro} = (a + a_1 \times MAT_{standardized} + a_2 \times \ln MAT_{standardized}) \times M^b$	(4)
$BCEF_{to} = (a + a_1 \times MAP/1000) \times M^b$	(5)

We developed the generalized model of the $BCEF_s$ for each component, including two different variables, as well as basic variables (stand variables) and covariates (abiotic factors). The fitting results in Tables 4 and 6 show that generalized models with abiotic factors were better than the basic models, indicating that the abiotic variables can explain the variation in $BCEF_s$.

Table 6. Fit Statistics of the Generalized Model.

	Index	Model (1)	Model (2)	Model (3)	Model (4)	Model (5)
parameter	a	0.746	0.018	0.018	0.554	1.131
	a_1	-0.214	0.227	-0.003	-0.356	-0.311
	a_2				0.151	
	b	-0.023	0.640	0.172	-0.048	-0.011
statistical index	R_a^2	0.393	0.709	0.264	0.561	0.295
	-2LL	-3997.374	-5994.685	-9721.432	-5692.578	-2982.493
	AIC	-3989.374	-5986.685	-9713.432	-5682.578	-2974.493
	RMSE	0.035	0.013	0.002	0.016	0.057

3.2. Mixed-Effects Models

Accounting for the random effects of FMU , we added random effects to the different parameters in the model, and mixed-effects models of position combinations of all random effects parameters were fitted. The UN structure was selected for the random effect variance-covariance matrix. For models with two or more random effects parameters, either the parameters were insignificant, or the models did not converge. In the convergent model, the AIC and $-2LL$ values were compared to determine whether the parameter estimation reached a significant level (Table 7). In addition to the $BCEF_{ro}$, we added random parameters to the intercept term in the model, and the mixed-effects models are given by:

Table 7 shows the final forms of the mixed-effects models, where a_1 and a_2 are the fixed-effects coefficients, u_1 is the random-effects coefficient. The model performance from the mixed-effects models significantly improved with a lower AIC and a larger R_a^2 than generalized models or basic models (Tables 4, 6 and 8). Obviously, the mixed-effects model performed better when dealing with hierarchical and nested data. There was no more obvious deviation of the residuals among the predicted $BCEF_s$, which used the

generalized models and mixed-effects models. Therefore, it was not necessary to eliminate heteroscedasticity (Figure 2).

Table 7. Mixed-effects model of biomass conversion and expansion factor of each component.

Mixed-Effects Model	Model
$BCEF_{st} = (a + u_1 + a_1 \times MAP/1000) \times M^b$	(6)
$BCEF_{br} = (a + u_1 + a_1 \times AHM/1000) \times Dq^b$	(7)
$BCEF_{fol} = (a + u_1 + a_1 \times ELV/1000) \times Dq^b$	(8)
$BCEF_{ro} = (a + a_1 \times MAT_{standardized} + (a_2 + u_1) \times \ln MAT_{standardized}) \times M^b$	(9)
$BCEF_{to} = (a + u_1 + a_1 \times MAP/1000) \times M^b$	(10)

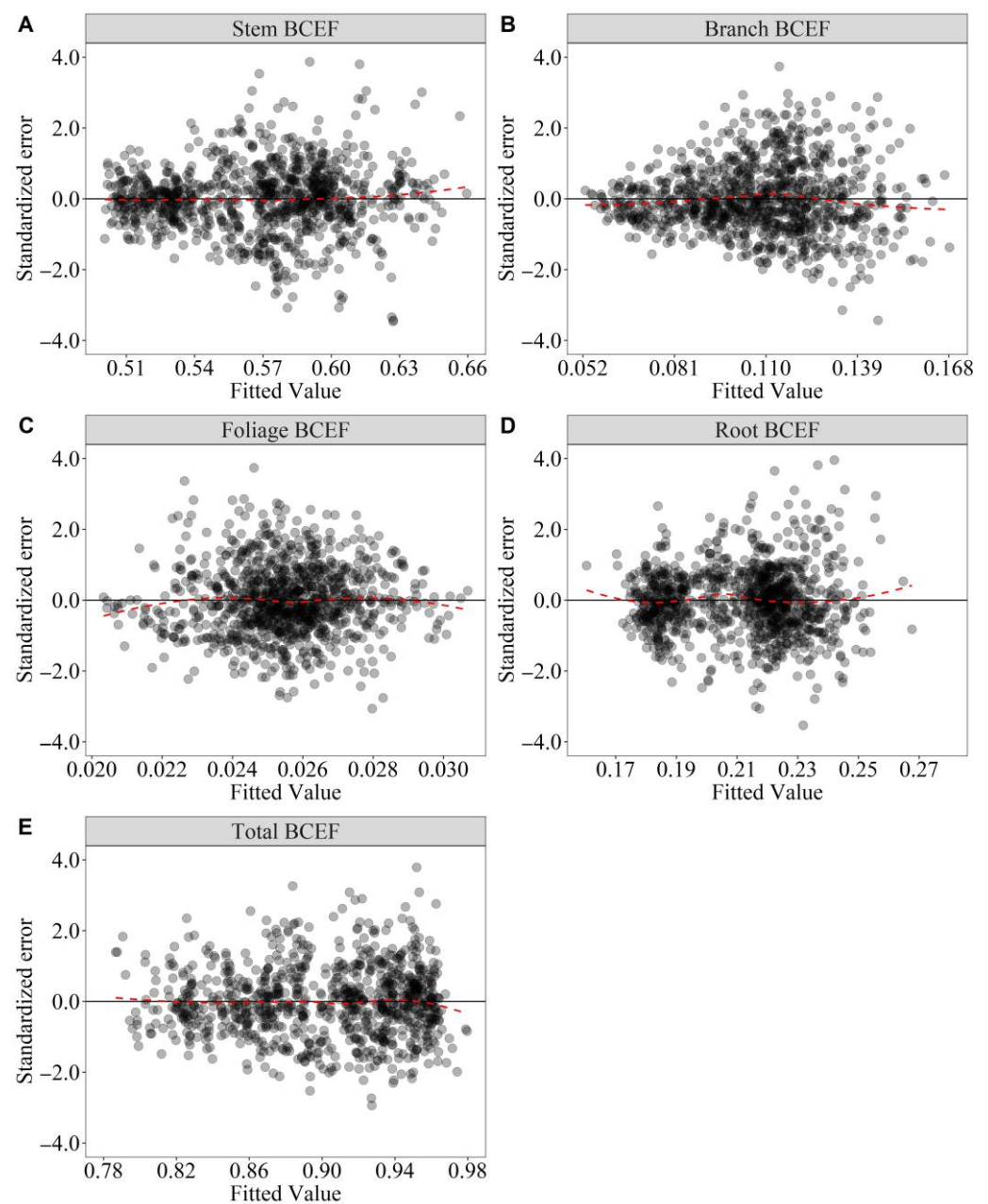


Figure 2. Standardized error plots for the mixed-effects models for $BCEF_s$ of five biomass components ((A): stem, (B): branch, (C): foliage, (D): root and (E):total) of the natural white birch forest.

Table 8. Fitting Statistics of the Mixed-Effects Model.

Index		Model (6)	Model (7)	Model (8)	Model (9)	Model (10)
fixed-effect	<i>a</i>	0.656	0.013	0.016	0.317	1.020
	<i>a</i> ₁	−0.083	0.161	−0.001	−0.081	−0.156
	<i>a</i> ₂				0.039	
	<i>b</i>	−0.016	0.760	0.193	−0.043	−0.004
random-effect	σ_{u1}	0.031	0.001	0.001	0.043	0.048
	σ	0.026	0.011	0.002	0.012	0.041
statistical index	R_a^2	0.676	0.791	0.445	0.749	0.648
	−2LL	−4478.723	−6201.959	−10048.370	−6070.187	−3533.493
	AIC	−4468.723	−6191.959	−.370	−6058.187	−3523.493
	RMSE	0.026	0.011	0.002	0.012	0.041

Note: σ_u is the standard deviation of the random effect parameter, and σ is the residual standard deviation.

Figure 3 presents trends of $BCEF_s$ for biomass components for different levels of model abiotic variables, which were the main effects, and the prediction of $BCEF$ of each component was performed via the fixed-effects model. The results showed that the different component $BCEF_s$ displayed significant relationships with different stand factors. $BCEF_{st}$, $BCEF_{ro}$ and $BCEF_{to}$ values began at a high level and decreased with increasing stocking volume. However, $BCEF_{br}$ and $BCEF_{fol}$ were positively correlated with D_q . In addition to biological factors, the $BCEF_s$ were sensitive to MAT , MAP , AHM and ELV . In view of the effects of abiotic variables on the $BCEF_s$ of each component, $BCEF_{st}$ and $BCEF_{to}$ decreased with increasing MAP . $BCEF_{br}$ increased with increasing AHM . $BCEF_{fol}$ decreased with increasing ELV . The responses of $BCEF_{ro}$ to MAT increased at first, and then decreased when MAT increased above $-0.5\text{ }^\circ\text{C}$.

3.3. Model Assessment and Calibration Prediction

Model validation was implemented using the jackknife residuals of the generalized models and mixed-effects models. The test results show that, for $MAPE$ and FE , the prediction performance of the mixed-effects models was better than that of the generalized models (Table 9). The predicted value was closer to the real observed value after being corrected by the random effect parameter.

Table 9. Testing Results of the Model of $BCEF_s$ for Natural White Birch Forest.

Component	Generalized Model			Mixed-Effect Model		
	MAE/Mg m ^{−3}	MAPE/%	FE	MAE/Mg m ^{−3}	MAPE/%	FE
stem	0.028	4.851	0.361	0.019	3.275	0.671
breach	0.011	10.138	0.689	0.009	8.033	0.790
foliage	0.002	7.297	0.233	0.002	6.011	0.436
root	0.012	5.808	0.522	0.009	4.167	0.742
total	0.046	5.050	0.254	0.032	3.487	0.643

The calculated random effect parameters differed depending on the size of the sample when the mixed-effects model was used for prediction. We randomly selected 1 to 16 plots from each FMU for FMU -level local calibration using $BLUPs$ theory, which was repeated continuously 500 times to calculate the average. Figure 4 displays that the $MAPE$ (%) changes across varied sample size for the mixed-effects model of each component. When the size of the sample was 0, it meant that only fixed parameters were used to calculate the predicted results. As seen in Figure 4, the $MAPE$ (%) of $BCEF_s$ of each component showed a decreasing trend with increasing sample numbers. However, when eight plots per FMU were sampled, the $MAPE$ (%) of the mixed-effects models tended to be stable. Our results indicated there were nonsignificant discrepancies among the evaluation statistical indicators, when the sampling number was larger than eight plots (Figure 4). Therefore, if

the survey cost and the prediction accuracy were comprehensively considered, eight plots would be selected from each *FMU* to correct the $BCEF_i$ of all plots of the *FMU*.

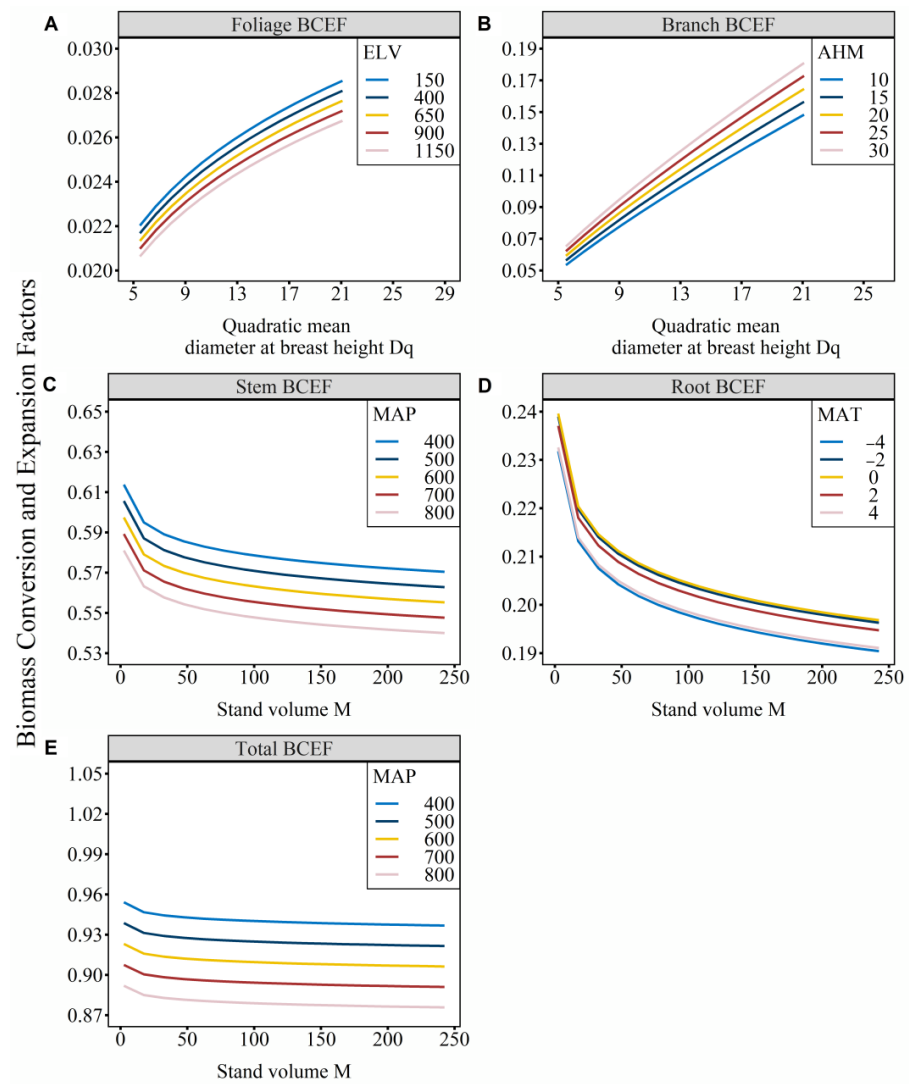


Figure 3. The variation in the $BCEF_s$ of five components ((A): branch, (B): foliage, (C): stem, (D): root and (E):total) along abiotic variable gradients.

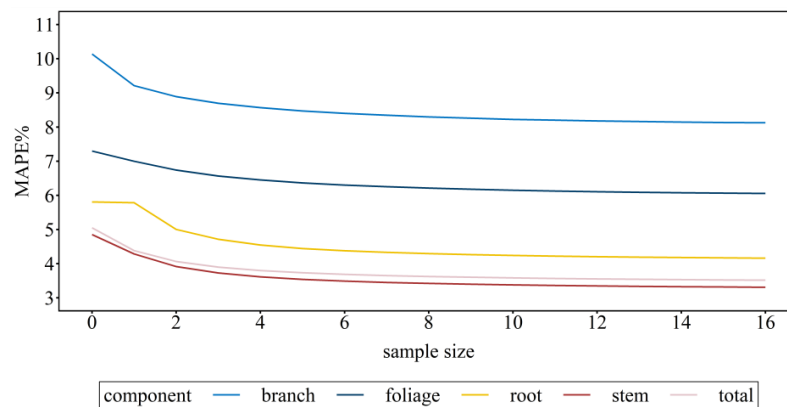


Figure 4. The effect of varying sampling sizes on the prediction of the mixed-effects model in 500 times random samples.

4. Discussion

In northeast China, natural white birch is one of the most dominant broad-leaved tree species, with a wide distribution and a fast growth rate as well as the potential to absorb large amounts of carbon, playing a significant role in the carbon balance of forest ecosystems [64–66]. The importance of the natural white birch forest in the carbon budgets and climatic system of northeastern China cannot be ignored. In the present study, the median value of the natural white birch forest total $BCEF_s$ for northern China was 0.7473 to 1.125 Mg m^{-3} , while a study in northern parts of Pakistan revealed that in the white birch forest the total $BCEF_s$ was 1.34 to 1.5 $\text{Mg}\cdot\text{m}^{-3}$ [67]. The values obtained in the study in the northern parts of Pakistan were slightly greater than those obtained in our study. However, a few studies in China [6,23] reported $BCEF_s$ of white birch and corroborated our observations. The study revealed that total $BCEF_s$ did not fall within the range specified by the IPCC for white birch trees. The total $BCEF_s$ ranged from 1.15 to 4.2 $\text{Mg}\cdot\text{m}^{-3}$, with a mean value of 1.3 $\text{Mg}\cdot\text{m}^{-3}$ [22]. However, the $BCEF_s$ is defined by the IPCC as the direct conversion of marketable growing stock into above-ground biomass, while the whole stem volume and whole biomass were used for calculation in our study, so that they cannot be compared directly [68]. If the IPCC default values were used, they would have produced varying degrees of error for estimates of China's forest carbon stocks. Consequently, we developed a variable $BCEF_s$ for biomass components suitable for northern China.

To improve the accuracy of carbon storage estimation in natural white birch forest in northeast China, in this paper, we first investigated the effect of stand characteristics on $BCEF_s$ for biomass components of natural white birch forest. Previously, a number of studies used age as an independent variable in the $BCEF_s$ model, but it cannot be easily measured in natural forests [29,69]. The major feature affecting $BCEF_{br}$ and $BCEF_{fol}$ was the quadratic mean diameter (D_q), and the most important feature influencing $BCEF_{st}$, $BCEF_{ro}$ and $BCEF_{to}$ was stocking volume (M) (Table 4). To a certain extent, the stand variables used in the model system of this paper were not only indirect substitutes for stand development but could also effectively reflected the growth differences of stands and the site index; this was also confirmed by Dong, et al. [6] and Jagodziński, et al. [69]. Table 4 shows that the parameter estimates for stocking volume (M) for the $BCEF_{st}$, $BCEF_{ro}$ and $BCEF_{to}$ models were negative and had the opposite sign as that for the quadratic mean diameter (D_q) for the $BCEF_{br}$ and $BCEF_{fol}$ models. It showed that $BCEF_{st}$, $BCEF_{ro}$ and $BCEF_{to}$ values decreased with increasing M . Figure 3B–D shows the decrease in $BCEF_{st}$, $BCEF_{ro}$ and $BCEF_{to}$ with tree size as the stand developed, tending to a constant value as the stand grew, which was also in agreement with the findings reported by other authors [23,29,52]. However, Jagodziński, et al. [10] used stocking volume (M) as the young naturally regenerated white birch for the $BCEF_s$ modeled independent variable, which led to the conclusion that $BCEF_s$ values had a preliminary increase in the stem biomass, and beyond the break point, the $BCEF_s$ stabilized and remained constant. This may be because the forest data we used were more mature than those used in his research, due to the differences of biomass allocation patterns during stand development and tree aging, the values formulated by old trees were not applicable for young trees [28,70]. In addition, Figure 3A,B shows that the $BCEF_{br}$ and $BCEF_{fol}$ values of the natural white birch forest increased with increasing quadratic mean diameter (D_q). Jagodziński, et al. [29] provided an overview of aboveground biomass estimates of young Scots pine in lowlands of western and central Poland and their results indicated that $BCEF_{br}$ and $BCEF_{fol}$ decreased with increasing age and tree diameter as the stand developed. This viewpoint is contrary to the research results on branches and foliage in this paper. In a study on biomass estimation of major forest types in the eastern Daxing'an Mountains, Dong, et al. [6] found that natural hardwood species biomass allocation, especially natural white birch forest, showed that the average proportion of stems and roots increased with decreasing diameter, while the average proportion of branches and leaves increased with increasing diameter.

Many studies have shown that temperature and precipitation can affect the distribution pattern of forest biomass [71,72]. As indicated by Luo, et al. [23], biomass conversion

and expansion factors have also been influenced by climate change. However, in our study, we found that the relationships between $BCEF_s$ and abiotic variables varied within different tree components (Figure 3). $BCEF_{st}$ and $BCEF_{to}$ generally decreased with increasing MAP . Similar results were reported by Luo, et al. [23], which can be explained by the fact that higher precipitation favors greater tree growth, lower wood density and leads to more increments allocated to tree stems. With the increasing of MAT , $BCEF_{ro}$ increased and then decreased. This result differed from that of Luo's study [23], which suggested that $BCEF_{ro}$ decreased with increasing MAT . The possible reason for this difference may be that with increasing temperature, the activity of microorganisms and the decomposition of forest litter can be promoted, thus promoting the growth of the root system [73]. However, the proportion of stem dry allocated biomass increased with the continued increase in temperature because the root biomass ratio was relatively reduced [74]. In the different compartments of biomass, the characteristics of branches determine the quantity of light interception and carbon dioxide assimilation, which are closely related to productivity [75]. The increasing trend of $BCEF_{br}$ with AHM (Figure 3) in the study can be attributed to the fact that an increase in AHM can lead to excessive temperature or increased evaporation, resulting in an increase in CMD , which limits the water absorption efficiency of vegetation [76]. This ultimately leads to a decline in the stem biomass and an increase in the branch biomass [23,77,78]. In addition, the elevation is an important topographic factor that indirectly affects stand growth and biomass allocation through its effects on water, nutrients, light, and topographic conditions [79,80]. The decreasing trend of $BCEF_{fol}$ with ELV (Figure 3) in the study suggested that the proportion of leaf biomass to total biomass decreased with increasing altitude, which was consistent with the findings of many earlier studies [81,82].

To derive strong inferences, we used the power function to describe the variations of $BCEF_s$ for different biomass components in the natural white birch forest. But the base model did not yield expected results. To further improve the performance of the model, we constructed the generalized model. In addition, this was because measurements were taken from the great mass of the sampling unit in the study. These measurements of different FUM were statistically correlated or different, not statistically independent; hence, the variance of the parameter may be underestimated using the ordinary least-squares techniques [3]. We used the nonlinear mixed-effects model to process the data in this paper. According to Tables 4, 6 and 8, the nonlinear mixed models for different components outperformed the base and generalized models in validation and fitting. FMU-level random effects in nonlinear mixed-effect models were suitable for explaining the high variability in $BCEF_s$ among FMUs. Fu, et al. [41] clarified that the difficulty for convergence of the mixed-effects model increases with the number of random parameters. In this study, when there were two or more random effect parameters, the convergence of the model was difficult to achieve, so that all models in this paper contained only a random parameter. There was not enough attention given to the nonlinear mixed-effects model of $BCEF$ in previous studies [83–88]. Generally, all the measured data were used to evaluate the prediction accuracy of the model and calculate the random effect parameters. However, it is challenging to measure $BCEF_s$ in all stands over a large area, while selecting a few stands for $BCEF_s$ measurement would be more convenient and efficient in forestry surveys and applications. Thus, the nonlinear mixed effect model was calibrated by random sampling. Many studies have found that larger sample sizes lead to better model performance [42]. Based on the significance test in Figure 4, when the sample size was eight, the prediction results achieved high accuracy. Therefore, when the sample size is limited to eight, the prediction accuracy can be ensured, and the workload can be reduced.

5. Conclusions

Understanding the sources of change in $BCEF_s$ can effectively reduce the uncertainties of stand biomass carbon estimates, which is a prerequisite for carbon stock estimation on a large regional scale.

We investigated for the first time the relationship between changes in $BCEF_s$ of natural white birch forest and stand development, climate, and topographic factors, and developed a nonlinear mixed-effects model including FMU random effects. The results showed the following: (i) there were significant variations between $BCEF_s$ and stand development (the quadratic mean diameter and standing volume), climate (mean annual temperature, mean annual precipitation and annual heat) and topographic factors (elevation), which should be considered when building the prediction model of $BCEF_s$; and (ii) the fitting results of the mixed-effects model outperformed the basic and generalized models. The biomass conversion and expansion factors ($BCEF_s$) presented here may be a beneficial tool for appraising the forest biomass and carbon sequestration of natural white birch forest.

When compared with earlier methods for estimation of $BCEF_s$, the strength of this study is as follows: (i) abiotic factors should be taken into account in developing predictive models of $BCEF_s$; (ii) equations for estimating natural white birch forest biomass and $BCEF$ for northern China were developed, which have lower uncertainties and are more systematic, because the mixed-effects model with random effects was used instead of least squares to estimate the model; and (iii) we can use a small sample size (sample size of eight sample) for prediction. However, the limitation of the present study is that it focused only on a natural white birch forest, and other species remain to be examined. We suggest that a dependable model of FUM-level $BCEF_s$ for different species be formulated based on existing data.

Author Contributions: Conceptualization, L.D.; Methodology, Z.M. and L.D.; Software, Y.W. and Z.M.; Validation, Y.W. and L.D.; Formal analysis, Y.W., Z.M. and L.D.; Investigation, F.L., Y.W., Y.H., Z.M. and L.D.; Resources, L.D.; Data curation, F.L., Y.W., Z.M., Y.H. and L.D.; Writing—original draft, Y.W.; Writing—review & editing, Y.W., Z.M., Y.H., L.D. and F.L.; Visualization, Y.W., Z.M. and Y.H.; Supervision, Y.W., Z.M., Y.H. and L.D.; Project administration, L.D. and F.L.; Funding acquisition, L.D. and F.L. All authors have read and agreed to the published version of the manuscript.

Funding: This research was supported by the National Key R&D Program of China, grant number 2022YFD2201001; the Joint Funds for Regional Innovation and Development of the National Natural Science Foundation of China, grant number U21A20244.

Data Availability Statement: The data presented in this study are available on request from the corresponding author. The data are not publicly available due to confidentiality.

Acknowledgments: The authors would like to thank the faculty and students of the Department of Forest Management, Northeast Forestry University (NEFU), China who provided and collected the data for this study.

Conflicts of Interest: The authors declare no conflict of interest.

References

1. Cui, J.; Lam, S.K.; Xu, S.; Lai, D.Y.F. The response of soil-atmosphere greenhouse gas exchange to changing plant litter inputs in terrestrial forest ecosystems. *Sci. Total Environ.* **2022**, *838*, 155995. [[CrossRef](#)] [[PubMed](#)]
2. Yang, L.; Niu, S.; Tian, D.; Zhang, C.; Liu, W.; Yu, Z.; Yan, T.; Yang, W.; Zhao, X.; Wang, J. A global synthesis reveals increases in soil greenhouse gas emissions under forest thinning. *Sci. Total Environ.* **2022**, *804*, 150225. [[CrossRef](#)] [[PubMed](#)]
3. Ma, A.; Miao, Z.; Xie, L.; Dong, L.-H.; Li, F. Crown width prediction for *Larix olgensis* plantations in Northeast China based on nonlinear mixed-effects model and quantile regression. *Trees* **2022**, *36*, 1761–17176. [[CrossRef](#)]
4. Singh, V.; Tewari, A.; Kushwaha, S.P.S.; Dadhwal, V.K. Formulating allometric equations for estimating biomass and carbon stock in small diameter trees. *For. Ecol. Manag.* **2011**, *261*, 1945–1949. [[CrossRef](#)]
5. Keith, H.; Lindenmayer, D.B.; Mackey, B.G.; Blair, D.; Carter, L.; McBurney, L.; Okada, S.; Konishi-Nagano, T. Accounting for Biomass Carbon Stock Change Due to Wildfire in Temperate Forest Landscapes in Australia. *PLoS ONE* **2014**, *9*, e107126. [[CrossRef](#)]
6. Dong, L.; Zhang, L.; Li, F. Evaluation of Stand Biomass Estimation Methods for Major Forest Types in the Eastern Da Xing'an Mountains, Northeast China. *Forests* **2019**, *10*, 715. [[CrossRef](#)]
7. IPCC. *Good Practice Guidance for Land Use. Land-Use Change and Forestry*; Penman Hayama, J., Ed.; IPCC National Greenhouse Gas Inventories Programme Technical Support Unit: Institute for Global Environmental Strategies: Kanagawa, Japan, 2003.
8. Canadell, J.; Ciais, P.; Cox, P.; Heimann, M. Quantifying terrestrial carbon sinks—Preface. *Clim. Chang.* **2004**, *67*, 145–146.
9. Canadell, J.G.; Raupach, M.R. Managing forests for climate change mitigation. *Science* **2008**, *320*, 1456–1457. [[CrossRef](#)] [[PubMed](#)]

10. Jagodziński, A.M.; Zasada, M.; Bronisz, K.; Bronisz, A.; Bijak, S. Biomass conversion and expansion factors for a chronosequence of young naturally regenerated silver birch (*Betula pendula* Roth) stands growing on post-agricultural sites. *For. Ecol. Manag.* **2017**, *384*, 208–220. [[CrossRef](#)]
11. Lehtonen, A.; Mäkipää, R.; Heikkinen, J.; Sievänen, R.; Liski, J. Biomass expansion factors (BEFs) for Scots pine, Norway spruce and birch according to stand age for boreal forests. *For. Ecol. Manag.* **2004**, *188*, 211–224. [[CrossRef](#)]
12. Teobaldelli, M.; Somogyi, Z.; Migliavacca, M.; Usoltsev, V.A. Generalized functions of biomass expansion factors for conifers and broadleaved by stand age, growing stock and site index. *For. Ecol. Manag.* **2009**, *257*, 1004–1013. [[CrossRef](#)]
13. Bruchwald, A.; Dmyterko, E.; Wojtan, R. Model wzrostu dla modrzewia europejskiego (*Larix decidua* Mill.) wykorzystujący cechy taksacyjne drzewostanu. *Leśne Pr. Badaw.* **2011**, *72*, 77–81.
14. Aholoukpe, H.; Dubos, B.; Flori, A.; Deleporte, P.; Amadji, G.; Chotte, J.L.; Blavet, D. Estimating aboveground biomass of oil palm: Allometric equations for estimating frond biomass. *For. Ecol. Manag.* **2013**, *292*, 122–129. [[CrossRef](#)]
15. Dong, L.; Zhang, L.; Li, F. Additive Biomass Equations Based on Different Dendrometric Variables for Two Dominant Species (*Larix gmelini* Rupr. and *Betula platyphylla* Suk.) in Natural Forests in the Eastern Daxing'an Mountains, Northeast China. *Forests* **2018**, *9*, 261. [[CrossRef](#)]
16. Dong, L.; Zhang, L.; Li, F. Developing additive systems of biomass equations for nine hardwood species in Northeast China. *Trees* **2015**, *29*, 1149–1163. [[CrossRef](#)]
17. Fayolle, A.; Doucet, J.L.; Gillet, J.F.; Bourland, N.; Lejeune, P. Tree allometry in Central Africa: Testing the validity of pantropical multi-species allometric equations for estimating biomass and carbon stocks. *For. Ecol. Manag.* **2013**, *305*, 29–37. [[CrossRef](#)]
18. Kuyah, S.; Dietz, J.; Muthuri, C.; Jamnadass, R.; Mwangi, P.; Coe, R.; Neufeldt, H. Allometric equations for estimating biomass in agricultural landscapes: II. Belowground biomass. *Agric. Ecosyst. Environ.* **2012**, *158*, 225–234. [[CrossRef](#)]
19. Ngomanda, A.; Engone Obiang, N.L.; Lebamba, J.; Moundounga Mavouroulou, Q.; Gomat, H.; Mankou, G.S.; Loumeto, J.; Midoko Iponga, D.; Kossi Ditsouga, F.; Zinga Koumba, R.; et al. Site-specific versus pantropical allometric equations: Which option to estimate the biomass of a moist central African forest? *For. Ecol. Manag.* **2014**, *312*, 1–9. [[CrossRef](#)]
20. Ter-Mikaelian, M.T.; Korzukhin, M.D. Biomass equations for sixty-five North American tree species. *For. Ecol. Manag.* **1997**, *97*, 1–24. [[CrossRef](#)]
21. Zuo, S.; Ren, Y.; Wang, X.; Zhang, X.; Luo, Y. Biomass Estimation Factors and Their Determinants of *Cunninghamia lanceolata* Forests in China. *Sci. Silvae Sin.* **2014**, *50*, 1–12.
22. IPCC. *2006 IPCC Guidelines for National Greenhouse Gas Inventories Volume 4 Agriculture, Forestry and Other Land Use*; IPCC: Geneva, Switzerland, 2006.
23. Luo, Y.; Zhang, X.; Wang, X.; Ren, Y. Dissecting Variation in Biomass Conversion Factors across China's Forests: Implications for Biomass and Carbon Accounting. *PLoS ONE* **2014**, *9*, e94777. [[CrossRef](#)]
24. Löwe, H.; Seufert, G.; Raes, F. Comparison of methods used within Member States for estimating CO₂ emissions and sinks according to UNFCCC and EU Monitoring Mechanism: Forest and other wooded land. *Biotechnol. Agron. Société Et Environ.* **2000**, *4*, 315–319.
25. Petersson, H.; Melin, Y. Estimating the biomass and carbon pool of stump systems at a national scale. *For. Ecol. Manag.* **2010**, *260*, 466–471. [[CrossRef](#)]
26. Chen, X.; Zhang, X.; Zhang, Y.; Wan, C. Carbon sequestration potential of the stands under the Grain for Green Program in Yunnan Province, China. *For. Ecol. Manag.* **2009**, *258*, 199–206. [[CrossRef](#)]
27. Lisboa, S.N.; Guedes, B.S.; Ribeiro, N.; Siteo, A. Biomass allometric equation and expansion factor for a mountain moist evergreen forest in Mozambique. *Carbon Balance Manag.* **2018**, *13*, 23. [[CrossRef](#)] [[PubMed](#)]
28. Krejza, J.; Svetlik, J.; Bednar, P. Allometric relationship and biomass expansion factors (BEFs) for above- and below-ground biomass prediction and stem volume estimation for ash (*Fraxinus excelsior* L.) and oak (*Quercus robur* L.). *Trees* **2017**, *31*, 1303–1316. [[CrossRef](#)]
29. Jagodziński, A.M.; Dyderski, M.K.; Gęsikiewicz, K.; Horodecki, P.; Cysewska, A.; Wierczyńska, S.; Maciejczyk, K. How do tree stand parameters affect young Scots pine biomass?—Allometric equations and biomass conversion and expansion factors. *For. Ecol. Manag.* **2018**, *409*, 74–83. [[CrossRef](#)]
30. Enes, T.; Fonseca, T. Biomass conversion and expansion factors are affected by thinning. *For. Syst.* **2014**, *23*, 438–447. [[CrossRef](#)]
31. Brown, S.; Lugo, A.E. Biomass of tropical forests: A new estimate based on forest volumes. *Science* **1984**, *223*, 1290–1293. [[CrossRef](#)] [[PubMed](#)]
32. Luo, Y.; Wang, X.; Zhang, X.; Zhu, J.; Zhang, Z.; Hou, Z. Biomass Estimation Factors of *Larix principis-rupprechtii* Plantations in Northern China. *Sci. Silvae Sin.* **2010**, *46*, 6–11.
33. Zhang, X.; Wang, Z.; Chhin, S.; Wang, H.; Duan, A.G.; Zhang, J. Relative contributions of competition, stand structure, age, and climate factors to tree mortality of Chinese fir plantations: Long-term spacing trials in southern China. *For. Ecol. Manag.* **2020**, *465*, 118103. [[CrossRef](#)]
34. Miao, Z.; Zhang, L.; Widagdo, F.R.A.; Dong, L.; Li, F. Modeling the number of the first- and second-order branches within the live tree crown of Korean larch plantations in Northeast China. *Can. J. For. Res.* **2021**, *51*, 704–719. [[CrossRef](#)]
35. Li, C. Application of Mixed Effects Models in Forest Growth Model. *Sci. Silvae Sin.* **2009**, *45*, 131–138.
36. Liu, X.; Hao, Y.S.; Widagdo, F.R.A.; Xie, L.F.; Dong, L.H.; Li, F.R. Predicting Height to Crown Base of *Larix olgensis* in Northeast China Using UAV-LiDAR Data and Nonlinear Mixed Effects Models. *Remote Sens.* **2021**, *13*, 1834. [[CrossRef](#)]

37. Calegario, N.; Daniels, R.; Maestri, R.; Neiva, R. Modeling dominant height growth based on nonlinear mixed-effects model: A clonal Eucalyptus plantation case study. *For. Ecol. Manag.* **2005**, *204*, 11–21. [[CrossRef](#)]
38. Sharma, M.; Parton, J. Height-diameter equations for boreal tree species in Ontario using a mixed-effects modeling approach. *For. Ecol. Manag.* **2007**, *249*, 187–198. [[CrossRef](#)]
39. Lindstrom, M.L.; Bates, D.M. Nonlinear mixed effects models for repeated measures data. *Biometrics* **1990**, *46*, 673–687. [[CrossRef](#)]
40. Hall, D.B.; Clutter, M. Multivariate multilevel nonlinear mixed effects models for timber yield predictions. *Biometrics* **2004**, *60*, 16–24. [[CrossRef](#)]
41. Fu, L.; Zhang, H.; Sharma, R.P.; Pang, L.; Wang, G. A generalized nonlinear mixed-effects height to crown base model for Mongolian oak in northeast China. *For. Ecol. Manag.* **2017**, *384*, 34–43. [[CrossRef](#)]
42. Calama, R.; Montero, G. Interregional nonlinear height-diameter model with random coefficients for stone pine in Spain. *Can. J. For. Res.* **2004**, *34*, 150–163. [[CrossRef](#)]
43. Han, Y.Y.; Huang, W.; Sun, T.; Lu, B.; Mao, Z.J. Soil organic carbon stocks and fluxes in different age stands of secondary *Betula platyphylla* in Xiaoxing'an Mountain, China. *Acta Ecol. Sin.* **2015**, *35*, 1460–1469.
44. Jiang, L.; Liu, Z. Structure Characteristics of Natural Birch Community and Species Diversity in Great Xing'an Mountains. *For. Enginee Ring* **2014**, *30*, 14–17.
45. Hou, L.; Sun, T.; Mao, Z.; Lv, H.; Zhao, J.; Song, Y. Litter Decomposition and Nutrient Dynamic of *Betula platyphylla* Secondary Forest with Different Stand Ages in Xiaoxing'an Mountains. *Bull. Bot. Res.* **2012**, *32*, 492–496.
46. Zhang, Y.; Mu, C.C.; Zheng, T.; Li, N.N. Ecosystem carbon storage of natural secondary birch forests in Xiaoxing'an Mountains of China. *J. Beijing For. Univ.* **2015**, *37*, 38–47.
47. Wang, X.; Zhao, D.; Liu, G.; Yang, C.; Teskey, R.O. Additive tree biomass equations for *Betula platyphylla* Suk. plantations in Northeast China. *Ann. For. Sci.* **2018**, *75*, 60. [[CrossRef](#)]
48. Dong, L.; Li, F.; Jia, W. Compatible Tree Biomass Models for Natural White Birch (*Betula platyphylla*) in Northeast China Forest Area. *Sci. Silvae Sin.* **2013**, *49*, 75–85.
49. Wykoff, W. A Basal Area Increment Model for Individual Conifers in the Northern Rocky Mountains. *For. Sci.* **1990**, *36*, 1077–1104.
50. Monserud, R.; Sterba, H. A basal area increment model for even-and uneven-aged forest stands in Austria. *For. Ecol. Manag.* **1996**, *80*, 57–80. [[CrossRef](#)]
51. Liu, Q.; Meng, S.; Zhou, H. *Tree Volume Tables of China*; China Forestry Publishing House: Beijing, China, 2017.
52. Zhu, W.; Xu, Y.; Wang, Z.; Du, A. Biomass Estimation Coefficient and Its Impacting Factors for Eucalyptus Plantation in China. *Sci. Silvae Sin.* **2020**, *56*, 1–11.
53. He, X.; Lei, X.D.; Dong, L.H. How large is the difference in large-scale forest biomass estimations based on new climate-modified stand biomass models? *Ecol. Indic.* **2021**, *126*, 107569. [[CrossRef](#)]
54. Wang, T.; Wang, G.; Innes, J.; Seely, B.; Chen, B. ClimateAP: An application for dynamic local downscaling of historical and future climate data in Asia Pacific. *Front. Agric. Sci. Eng.* **2017**, *4*, 448–458. [[CrossRef](#)]
55. Butte, W.; Blum, J.K. Calculation of bioconcentration factors from kinetic data by non-linear iterative least-squares regression analysis using a programmable minicalculator. *Chemosphere* **1984**, *13*, 151–160. [[CrossRef](#)]
56. Inoue, K. Iterative weighted least-squares estimates in a heteroscedastic linear regression model. *J. Stat. Plan. Inference* **2003**, *110*, 133–146. [[CrossRef](#)]
57. Qiu, H.; Liu, S.; Zhang, Y.; Li, J. Variation in height-diameter allometry of ponderosa pine along competition, climate, and species diversity gradients in the western United States. *For. Ecol. Manag.* **2021**, *497*, 119477. [[CrossRef](#)]
58. Vizcaino-Palomar, N.; Ibanez, I.; Benito-Garzon, M.; Gonzalez-Martinez, S.C.; Zavala, M.A.; Alia, R. Climate and population origin shape pine tree height-diameter allometry. *New For.* **2017**, *48*, 363–379. [[CrossRef](#)]
59. Tian, D.; Jiang, L.; Shahzad, M.K.; He, P.; Wang, J.; Yan, Y. Climate-sensitive tree height-diameter models for mixed forests in Northeastern China. *Agric. For. Meteorol.* **2022**, *326*, 109182. [[CrossRef](#)]
60. Dong, L.; Widagdo, F.R.A.; Xie, L.; Li, F. Biomass and Volume Modeling along with Carbon Concentration Variations of Short-Rotation Poplar Plantations. *Forests* **2020**, *11*, 780. [[CrossRef](#)]
61. Harris, D.L.; Lofgren, D.L.; Stewart, T.S.; Schinckel, A.P. Adapting best linear unbiased prediction (BLUP) for timely genetic evaluation: I. Progeny traits in a single contemporary group for each sex. *J. Anim. Sci.* **1989**, *67*, 3209–3222. [[CrossRef](#)]
62. Nothdurft, A.; Saborowski, J.; Breidenbach, J. Spatial prediction of forest stand variables. *Eur. J. For. Res.* **2009**, *128*, 241–251. [[CrossRef](#)]
63. Viana, J.M.S.; Mundim, G.B.; Delima, R.O.; Silva, F.F.E.; De Resende, M.D.V. Best linear unbiased prediction for genetic evaluation in reciprocal recurrent selection with popcorn populations. *J. Agric. Sci.* **2014**, *152*, 428–438. [[CrossRef](#)]
64. Wang, X.W.; Weng, Y.H.; Liu, G.F.; Krasowski, M.J.; Yang, C.P. Variation in carbon concentration, sequestration and partitioning among white birch (*Betula platyphylla*) provenances. *For. Ecol. Manag.* **2015**, *358*, 344–352. [[CrossRef](#)]
65. Yao, P.; Chen, X.; Zhou, Y.; Zhao, W.; Lu, M.; Tu, J. Carbon sequestration potential of the major stands under the Grain for Green Program in Southwest China in the next 50 years. *Acta Ecol. Sin.* **2014**, *34*, e0150992.
66. Fang, J.; Liu, G.; Zhu, B.; Wang, X.; Liu, S. Carbon budgets of three temperate forest ecosystems in Dongling Mt., Beijing, China. *Sci. China Ser. D Earth Sci.* **2007**, *50*, 92–101. [[CrossRef](#)]
67. Syed Moazzam, N.; Alam, K. Assessing Biomass Expansion Factor of Birch Tree *Betula utilis* D. DON. *Open J. For.* **2014**, *4*, 181–190.

68. Eggleston, S.; Buendia, L.; Miwa, K.; Ngara, T.; Tanabe, K. 2006 IPCC Guidelines for National Greenhouse Gas Inventories. V.4. Agriculture, Forestry and Other Land Use; IPCC: Geneva, Switzerland, 2006.
69. Jagodziński, A.M.; Dyderski, M.; Gęsikiewicz, K.; Horodecki, P. Tree and stand level estimations of *Abies alba* Mill. aboveground biomass. *Ann. For. Sci.* **2019**, *76*, 56. [[CrossRef](#)]
70. Wirth, C.; Schumacher, J.; Schulze, E.D. Generic biomass functions for Norway spruce in Central Europe—A meta-analysis approach toward prediction and uncertainty estimation. *Tree Physiol.* **2004**, *24*, 121–139. [[CrossRef](#)]
71. Yu, M.; Liu, X.; Xue, L. Progress on effects of temperature and precipitation on forest biomass allocation patterns. *Ecol. Sci.* **2021**, *40*, 204–209.
72. Guo, J.; Guo, Y.; Chai, Y.; Liu, X.; Yue, M. Shrubland biomass and root-shoot allocation along a climate gradient in China. *Plant Ecol. Evol.* **2021**, *154*, 5–14. [[CrossRef](#)]
73. Zhou, L.; Li, B.G.; Zhou, G.S. ADVANCES IN CONTROLLING FACTORS OF SOIL ORGANIC CARBON. *Adv. Earth Sci.* **2005**, *20*, 99–105.
74. Fang, Y.; Zou, X.; Lie, Z.; Xue, L. Variation in Organ Biomass with Changing Climate and Forest Characteristics across Chinese Forests. *Forests* **2018**, *9*, 521. [[CrossRef](#)]
75. Poorte, A.; Nagel, O. The role of biomass allocation in the growth response of plants to different levels of light, CO₂, nutrients and water: A quantitative review. *IMF Occas. Pap.* **2000**, *27*, 595–607.
76. Ciais, P.; Reichstein, M.; Viovy, N.; Granier, A.; Ogee, J.; Allard, V.; Aubinet, M.; Buchmann, N.; Bernhofer, C.; Carrara, A.; et al. Europe-wide reduction in primary productivity caused by the heat and drought in 2003. *Nature* **2005**, *437*, 529–533. [[CrossRef](#)] [[PubMed](#)]
77. He, X.; Lei, X.; Zeng, W.; Feng, L.; Zhou, C.; Wu, B. Quantifying the Effects of Stand and Climate Variables on Biomass of Larch Plantations Using Random Forests and National Forest Inventory Data in North and Northeast China. *Sustainability* **2022**, *14*, 5580. [[CrossRef](#)]
78. Luo, Y.; Wang, X.; Zhang, X.; Ren, Y.; Poorter, H. Variation in biomass expansion factors for China's forests in relation to forest type, climate, and stand development. *Ann. For. Sci.* **2013**, *70*, 589–599. [[CrossRef](#)]
79. Wang, G.; Guan, D.; Xiao, L.; Peart, M.R. Forest biomass-carbon variation affected by the climatic and topographic factors in Pearl River Delta, South China. *J. Environ. Manag.* **2019**, *232*, 781–788. [[CrossRef](#)]
80. Konopka, B.; Pajtik, J.; Seben, V. Biomass functions and expansion factors for young trees of European ash and Sycamore maple in the Inner Western Carpathians. *Austrian J. For. Sci.* **2015**, *132*, 1–26.
81. Zhang, W.; Li, H.; Li, J.; Lu, Z.; Liu, G. Individual and modular biomass dynamics of *Kingdonia uniflora* population in Qinling Mountain. *J. Appl. Ecol.* **2003**, *14*, 530–534.
82. Guo, Z.; Lin, H.; Chen, S.; Yang, Q. Altitudinal Patterns of Leaf Traits and Leaf Allometry in Bamboo *Pleuroblastus amarus*. *Front. Plant Sci.* **2018**, *9*, 1110. [[CrossRef](#)]
83. Brown, S. Measuring carbon in forests: Current status and future challenges. *Environ. Pollut.* **2002**, *116*, 363–372. [[CrossRef](#)]
84. Turner, D.P.; Koerper, G.J.; Harmon, M.E.; Lee, J.J. A Carbon Budget for Forests of the Conterminous United States. *Ecol. Appl.* **1995**, *5*, 421–436. [[CrossRef](#)]
85. Schroeder, P.; Brown, S.; Mo, J.; Birdsey, R.; Cieszewski, C. Biomass estimation for temperate broadleaf forests of the United States using inventory data. *For. Sci.* **1997**, *43*, 424–434.
86. Albaugh, T.J.; Bergh, J.; Lundmark, T.; Nilsson, U.; Stape, J.L.; Allen, H.L.; Linder, S. Do biological expansion factors adequately estimate stand-scale aboveground component biomass for Norway spruce? *For. Ecol. Manag.* **2009**, *258*, 2628–2637. [[CrossRef](#)]
87. Petersson, H.; Holm, S.; Ståhl, G.; Alger, D.; Fridman, J.; Lehtonen, A.; Lundström, A.; Mäkipää, R. Individual tree biomass equations or biomass expansion factors for assessment of carbon stock changes in living biomass—A comparative study. *For. Ecol. Manag.* **2012**, *270*, 78–84. [[CrossRef](#)]
88. Soares, P.; Tomé, M. Biomass expansion factors for *Eucalyptus globulus* stands in Portugal. *For. Syst.* **2012**, *21*, 141–152. [[CrossRef](#)]

Disclaimer/Publisher's Note: The statements, opinions and data contained in all publications are solely those of the individual author(s) and contributor(s) and not of MDPI and/or the editor(s). MDPI and/or the editor(s) disclaim responsibility for any injury to people or property resulting from any ideas, methods, instructions or products referred to in the content.